

Solvation-Dependent Switching of Solid-state Luminescence of a Fluorinated Aromatic Tetrapyrazole

Zhenglin Zhang, Thien Lieu, Chia-Hua Wu, Xiqu Wang, Judy I. Wu, Olafs Daugulis, and Ognjen Š. Miljanić*

Department of Chemistry, University of Houston, 112 Fleming Building, Houston, Texas 77204-5003, United States

Email: miljanic@uh.edu

Phone: +1.832.842.8827

Web: www.miljanicgroup.com

Supporting Information

General Methods and Materials	S2
Synthesis of Precursors to the Targeted Fluorophore	S3
NMR and Mass Spectra of New Compounds	S7
Preparation of Crystals 1A and 1B	S13
Data of Absorption and Emission Spectra in THF/H₂O	S14
Photos and Excitation spectra of Wetting/Drying Cycles	S15
Single and Powder X-ray Diffusion Analysis	S17
Theoretical Calculations	S24
References	S25

General Methods and Materials

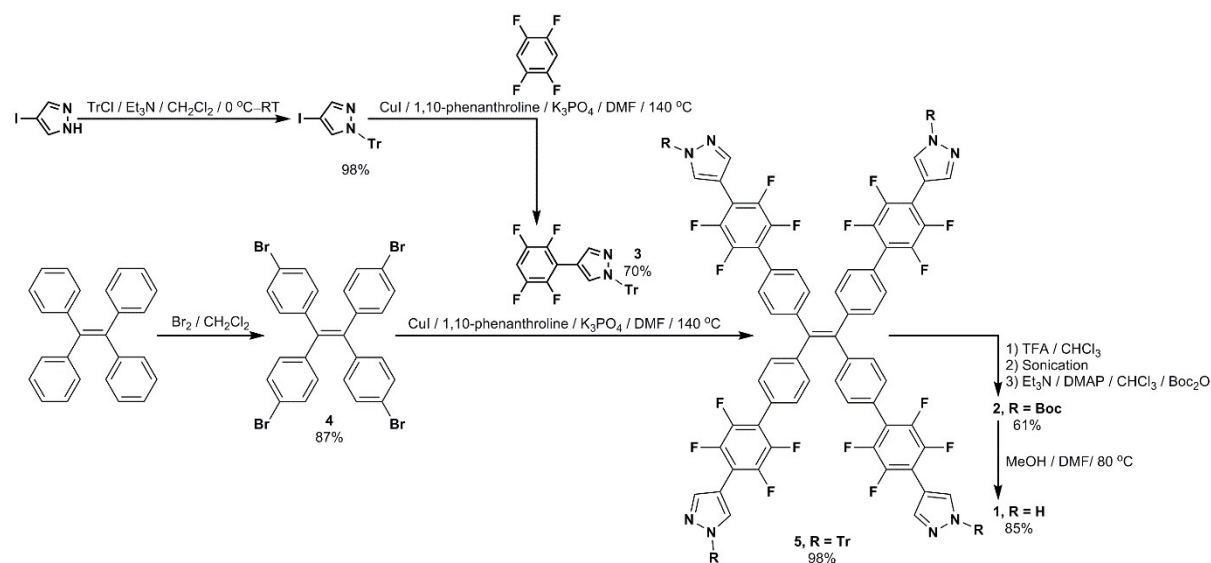
The ^1H and ^{19}F NMR spectra were obtained on JEOL ECA-600 and ECA-500 spectrometers, with working frequencies of 600 and 500 MHz, respectively (for ^1H nuclei), and using the peaks of residual solvent as standards. Mass spectra of unknown compounds were collected at the University of Texas at Austin Mass Spectrometry Facility. Infrared spectra were collected on a Nicolet iS10 FT-IR spectrometer. The absorption, emission, and excitation spectra were measured by using a PerkinElmer LAMBDA 25 UV/VIS spectrometer and a PerkinElmer LS 55 Fluorescence spectrometer. All the Calculations were carried out by Gaussian 16 program package. All pictures and video were taken by Canon EOS Rebel T3i. A microscope of Nikon SMZ-U with an external light source of a Leica KL 1500 LCD Fiber Optic Illuminator and an UVLS-28 UV lamp was used for the microscope photos.

All reactions were performed under nitrogen atmosphere in oven-dried glassware. The following starting materials and solvents were obtained from the respective commercial sources and used without further purification: 4-iodopyrazole, triethylamine (Et_3N), Boc_2O , hydroxylamine hydrochloride, 1,10-phenanthroline, tetraphenylethylene, trifluoroacetic acid (TFA), CH_2Cl_2 , CHCl_3 , MgSO_4 , NaHCO_3 , K_3PO_4 , NH_4Cl , 4-dimethylaminopyridine (DMAP), Br_2 , silica gel, hexane; ethyl acetate, EtOH (Sigma Aldrich); triphenylchloromethane (TrCl, AK Scientific); *N,N*-dimethyl formaldehyde (DMF, Sigma Aldrich and spectrometric grade of J. T. Baker); CuI (Strem); MeOH (Fisher Chemical); tetrahydrofuran (THF, spectrometric grade, Macron Fine Chemicals); and H_2O (spectrometric grade, Macron Fine Chemicals). K_3PO_4 was activated at 150 °C under nitrogen atmosphere for 1 day before using.

Experiments are presented in the order following the discussion of the manuscript.

Compound numbers are identical to those in the main text of the manuscript.

Synthesis of Precursors to the Targeted Fluorophore



Scheme S1. Synthetic route to compound 1.

N-trityl-4-iodopyrazole

Compound 4-iodopyrazole (19.4 g, 100 mmol) was dissolved in the mixture of dry CH₂Cl₂ (250 mL) and Et₃N (27.9 mL, 200 mmol) under a nitrogen atmosphere. The solution was cooled down in an ice bath (5 °C, inside the flask) and TrCl (30.7 g, 110 mmol) was added in ten portions over 20 min. The cooling bath was removed, and the mixture was stirred overnight. The mixture was poured into H₂O (200 mL) and NaHCO₃ (saturated aq. solution, 200 mL) was added slowly. The suspension was extracted with CH₂Cl₂ (4 × 150 mL), dried over MgSO₄, filtered, and evaporated. The product was purified using silica gel chromatography (dry loading) with hexanes/ethyl acetate mixture (9/1) as the eluent. After the removal of the solvent, the title compound was obtained as a white solid. Yield 42.7 g (98 %). This compound is known.¹

¹H NMR (CDCl₃, 500 MHz) δ 7.67 (s, 1H), 7.41 (s, 1H), 7.33–7.31 (m, 9H), 7.14–7.10 (m, 6H) ppm.

Compound 3

A pressure vessel was charged with *N*-trityl-4-iodopyrazole (32.7 g, 75.0 mmol) and 1,2,4,5-tetrafluorobenzene (16.75 ml, 150 mmol) at room temperature. The vessel was then placed in the glove box. After that, CuI (1.43 g, 7.5 mmol), 1,10-phenanthroline (1.35 g, 7.5 mmol), K₃PO₄ (31.8 g, 150 mmol), and DMF (45 mL) were added. The vessel was sealed, taken out of the glove box, and placed in an oil bath where it was heated at 140 °C for 36 h.

Subsequently, the reaction mixture was diluted with CHCl_3 (300 mL) and filtered through a Büchner filter. The solid was washed three times with CHCl_3 (3×100 mL). The combined filtrate was washed with concentrated aqueous NH_4Cl (3×400 mL) followed by drying over MgSO_4 , filtration and evaporation. The product was purified using silica gel chromatography (dry loading) with hexanes/ethyl acetate mixture (9/1) as the eluent. The title compound was obtained as a light yellow solid in the yield of 24 g (70 %). This compound is known.¹

^1H NMR (CDCl_3 , 600 MHz) δ 8.15 (s, 1H), 7.91 (s, 1H), 7.36–7.29 (m, 9H), 7.21–7.16 (m, 6H), 6.93–6.84 (m, 1H) ppm. ^{19}F NMR (470 MHz) δ -139.7 to -139.9 (m, 2F), -141.1 to -141.3 (m, 2F) ppm.

Compound 4

Compound 4 was obtained following a literature procedure.² Tetraphenylethylene (3.32 g, 10 mmol) was dissolved in CH_2Cl_2 (100 mL) in a round-bottom flask, followed by the dropwise addition of Br_2 (4 mL) in CH_2Cl_2 (20 mL) via syringe. The mixture was stirred at room temperature for 12 h, and then quenched with a saturated aqueous solution of hydroxylamine hydrochloride (100 mL). The aqueous solution was then extracted with an equal volume of CH_2Cl_2 . The organic layer was dried over MgSO_4 , filtered, and evaporated. The resulting solid was washed with EtOH (50 mL) to yield the title compound as a white powder (5.6 g, 87 %).

^1H NMR (CD_2Cl_2 , 600 MHz) δ 7.26 (d, $J = 6.0$ Hz, 8H), 6.85 (d, $J = 6.0$ Hz, 8H) ppm.

Compound 5

To a 150 mL pressure vessel, compounds 3 (24.7 g, 54 mmol) and 4 (7.80 g, 12 mmol) were added at room temperature. The vessel was then placed in glove box. After that, CuI (1.15 g, 6.0 mmol), 1,10-phenanthroline (1.1 g, 6.0 mmol), K_3PO_4 (13.1 g, 62 mmol), and DMF (48 mL) were added to the pressure vessel. The vessel was sealed and taken out of the glove box followed by placing in oil bath at 140 °C for 36 h. Subsequently, the reaction mixture was diluted with CHCl_3 (1.5 L) and filtered through a Büchner filter. The solid was then washed with CHCl_3 (3×100 mL). The combined filtrate was washed with concentrated aqueous NH_4Cl (3×1 L) followed by drying over MgSO_4 , filtration, and evaporation. The product was purified using silica gel chromatography (dry loading) with hexane/ethyl acetate mixture (95/5), followed by a CHCl_3 /EtOAc mixture (9/1) as the eluent. Yield 25.4 g (98 %) of a light-yellow solid, $R_f = 0.85$ (SiO_2 , CHCl_3 /EtOAc = 9/1), melting at 197–212 °C with decomposition.

^1H NMR (CD_2Cl_2 , 600 MHz) δ 8.10 (s, 4H), 7.91 (s, 4H), 7.33–7.29 (m, 44H), 7.23 (d, J = 8.2 Hz, 8H), 7.17–7.15 (m, 24H) ppm. ^{19}F NMR (565 MHz) δ –142.27 to –142.33 (m, 8F), –145.72 to –145.78 (m, 8F) ppm. HRMS (ESI) calcd. for $\text{C}_{138}\text{H}_{84}\text{F}_{16}\text{N}_8$ $[\text{M}+2\text{Na}]^{2+}$: 1101.8190; found: 1101.8219. FT-IR (neat, cm^{-1}) $\bar{\nu}$ 3057, 3033, 1651, 1597, 1563, 1516, 1480, 1445, 1115. Anal. Calc'd for $\text{C}_{138}\text{H}_{84}\text{F}_{16}\text{N}_8$: C, 76.80; H, 3.92; N, 5.19. Found: C, 76.59; H, 3.96; N, 5.27.

Compound 2

To a flame-dried round bottom flask was added compound **5** (25.4 g, 11.8 mmol) followed by CHCl_3 (300 mL). TFA (18.1 mL, 236 mmol) was added in one portion. The flask was sealed with a septum and the mixture was stirred at room temperature for one day. After that, the mixture was diluted with hexanes (300 mL) and stirred for 15 min. Precipitate was formed and filtered followed by washing with CHCl_3 (3 \times 50 mL) and hexane (3 \times 100 mL). After that, collected precipitate was dried under nitrogen atmosphere and vacuum for one day. The solid was then suspended in CHCl_3 (250 mL) and sonicated overnight. This step removes trityl groups, and the obtained product is very insoluble.

To a flame-dried Schlenk flask containing CHCl_3 (1 L) was added the crude product obtained in previous step. Et_3N (60 mL) was added in one portion and the suspension was stirred for 15 min, followed by adding DMAP (11.6 g, 95 mmol) and Boc_2O (40.0 g, 183 mmol). The suspension was stirred until clear solution was formed, followed by evaporation of volatiles. Purification by silica gel chromatography (dry loading) with CHCl_3 /ethyl acetate solvent mixture (9/1) as the eluent gave 11.5 g (61%) of a light-yellow solid, R_f = 0.75 (SiO_2 , chloroform/ethyl acetate = 9/1), mp: 408–417 $^\circ\text{C}$ with decomposition.

^1H NMR (CD_2Cl_2 , 600 MHz) δ 8.57 (s, 4H), 8.15 (s, 4H), 7.35 (d, J = 8.2 Hz, 8H), 7.28 (d, J = 8.2 Hz, 8H), 1.64 (s, 9H) ppm. ^{19}F NMR (470 MHz) δ –141.53 to –141.60 (m, 8F), –144.88 to –144.95 (m, 8F). HRMS (ESI) calcd. for $\text{C}_{82}\text{H}_{60}\text{F}_{16}\text{N}_8\text{O}_8$ $[\text{M}+2\text{Na}]^{2+}$: 817.2032; found: 817.2018. FT-IR (neat, cm^{-1}) $\bar{\nu}$ 3057, 2981, 2935, 1758, 1738, 1686, 1570, 1519, 1479, 1449, 1249, 1150, 1112. Anal. Calc'd for $\text{C}_{82}\text{H}_{60}\text{F}_{16}\text{N}_8\text{O}_8$: C, 61.97; H, 3.81; N, 7.05. Found: C, 61.94; H, 3.74; N, 7.16.

Compound 1

Compound 2 (300 mg, 0.19 mmol) was added to a 500 mL bottle. Solvent DMF (30 mL) and MeOH (270 mL) was added into the bottle and the bottle was capped, which was mixed for 10 min by a vortex mixer, and sonicated for 10 min, and then placed in an oven (80 °C) for 24 h. After cooling down to room temperature, the formed precipitate was filtered, washed with MeOH, and air dried to yield a yellow solid (191 mg, 85%), mp: 377–386 °C with decomposition.

^1H NMR (DMSO- d_6 , 600 MHz) δ 13.46 (s, 4H), 8.28 (s, 4H), 7.95 (s, 4H), 7.40 (d, J = 8.1 Hz, 8H), 7.25 (d, J = 8.1 Hz, 8H) ppm. ^{19}F NMR (DMSO- d_6 , 565 MHz) δ -141.82 to -141.88 (m, 8F), -144.91 to -144.97 (m, 8F) ppm. HRMS (ESI) calcd. for $\text{C}_{62}\text{H}_{28}\text{F}_{16}\text{N}_8$ $[\text{M}+\text{H}]^+$: 1189.2254; found: 1189.2253. FT-IR (neat, cm^{-1}) $\bar{\nu}$ 3465, 3146, 3072, 1652, 1569, 1517, 1467, 1264, 1222, 1147, 1049. Anal. Calc'd for $\text{C}_{62}\text{H}_{28}\text{F}_{16}\text{N}_8 \cdot 2\text{H}_2\text{O}$: C, 60.79; H, 2.63; N, 9.15. Found: C, 60.56; H, 2.48; N, 8.83.

NMR and Mass Spectra of New Compounds

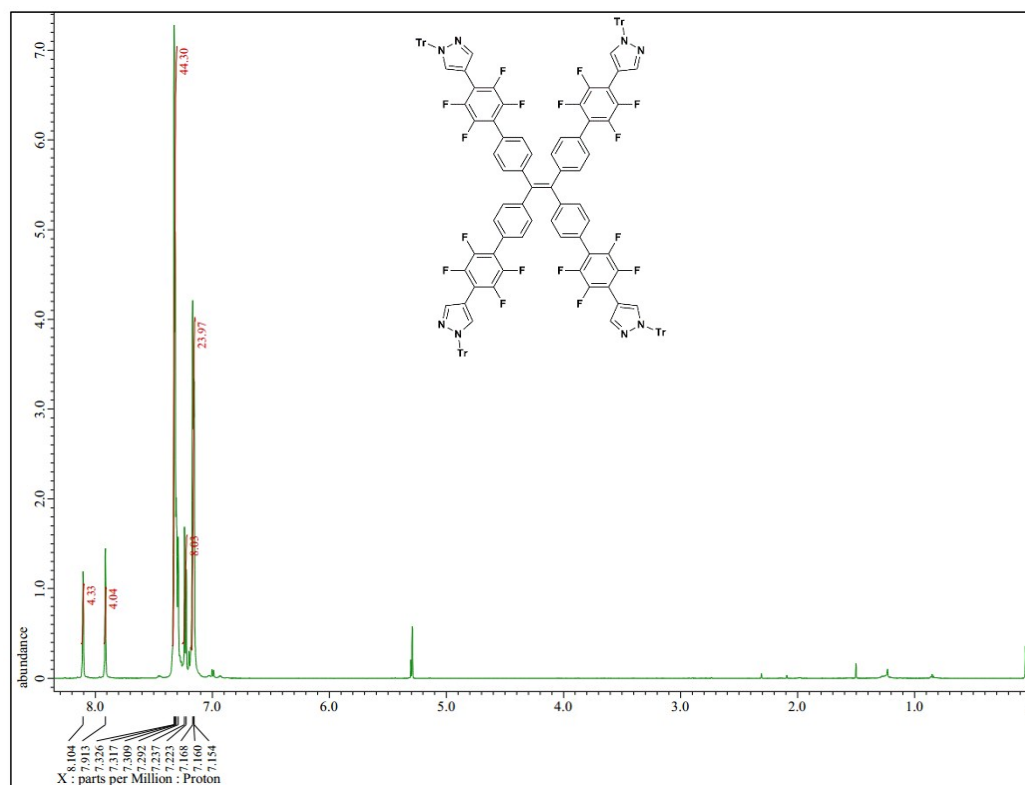


Figure S1. ¹H NMR spectrum of compound 5.

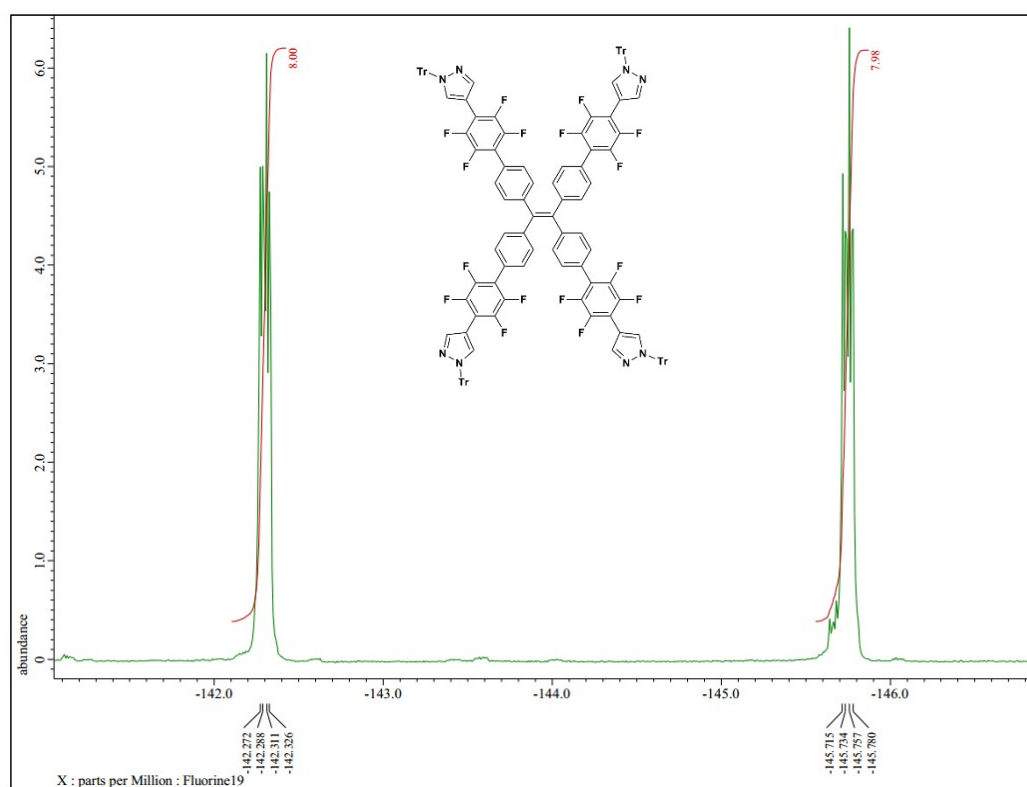


Figure S2. ¹⁹F NMR spectrum of compound 5.

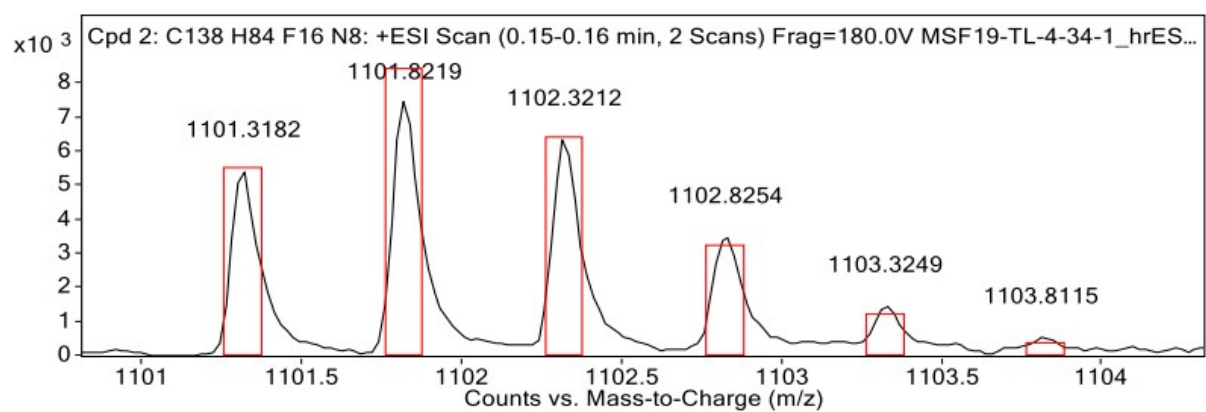


Figure S3. High-resolution mass spectrum of compound **5**.

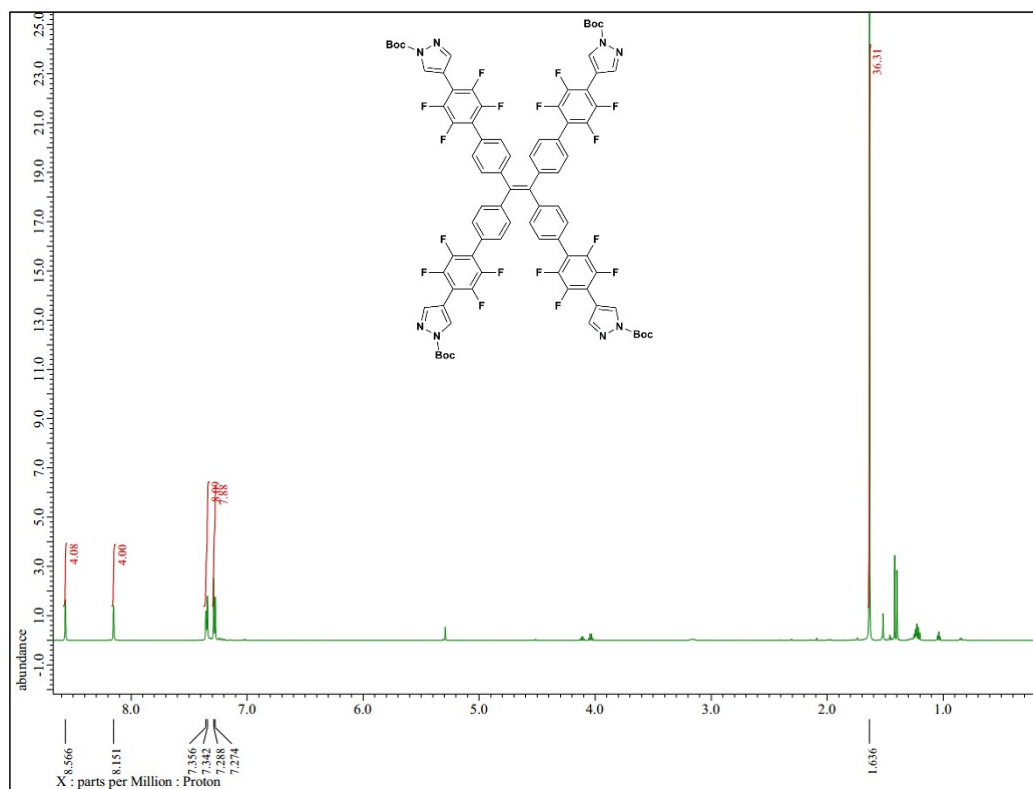


Figure S4. ¹H NMR spectrum of compound 2.

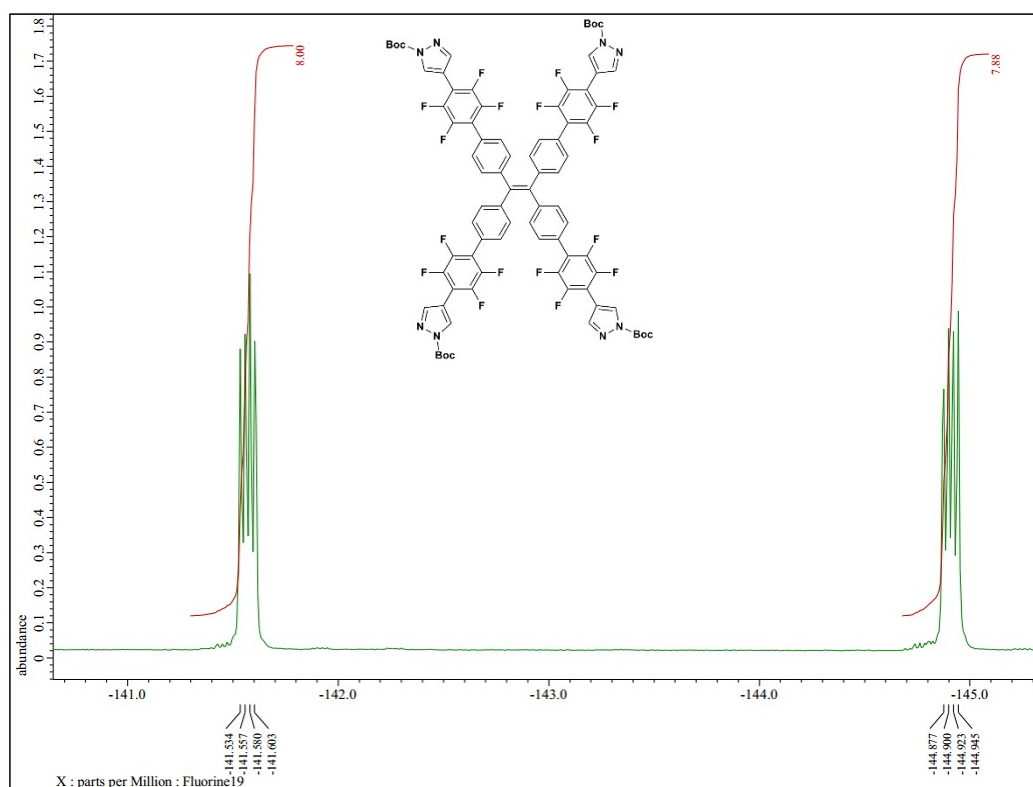


Figure S5. ¹⁹F NMR spectrum of compound 2.

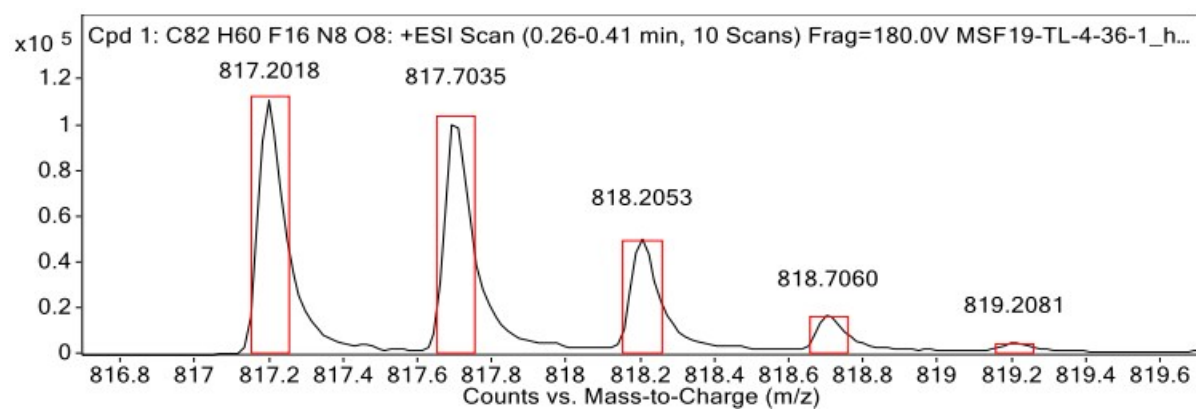


Figure S6. High-resolution mass spectrum of compound **2**.

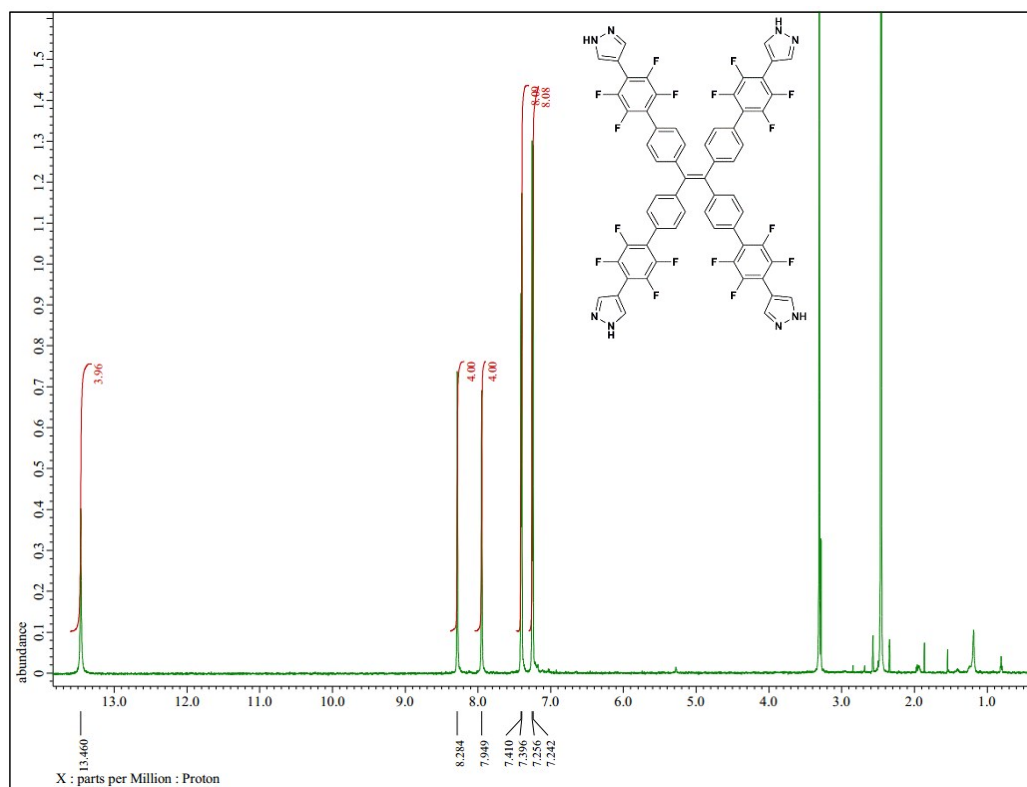


Figure S7. ^1H NMR spectrum of compound 1.

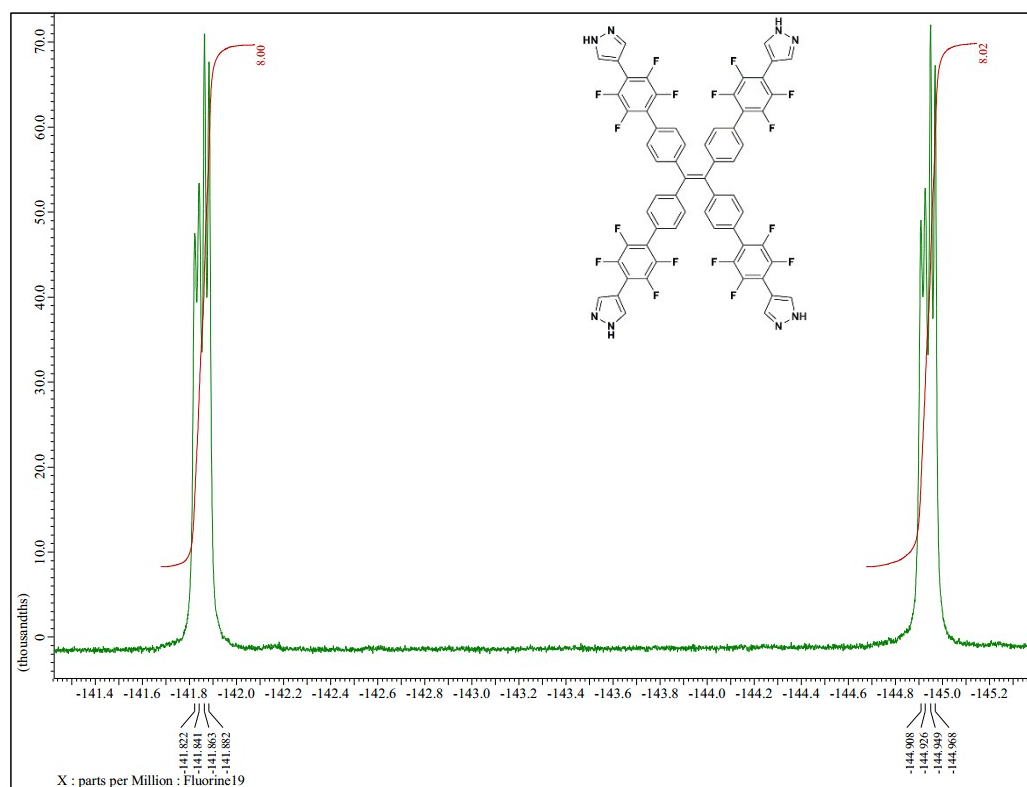


Figure S8. ^{19}F NMR spectrum of compound 1.

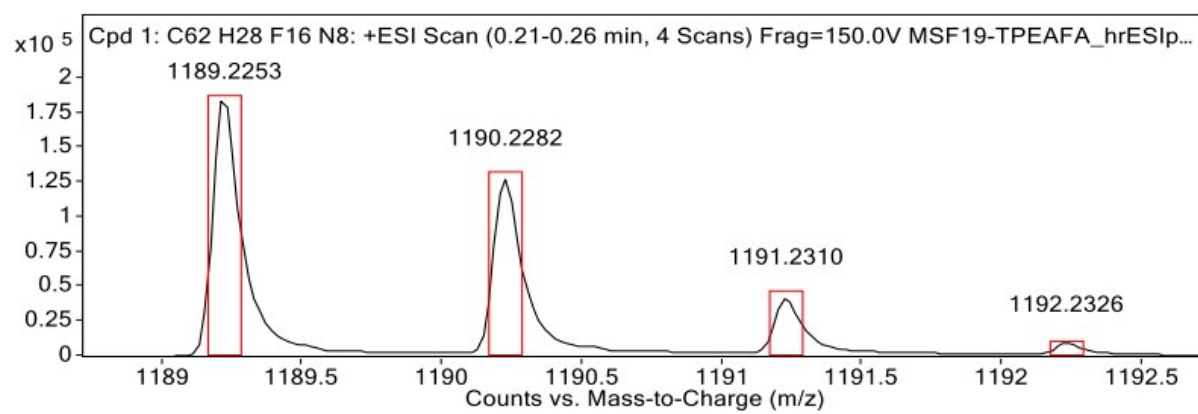


Figure S9. High-resolution mass spectrum of compound **1**.

Preparation of Crystals 1A and 1B

Crystal 1A

Compound **2** (400 mg, 0.25 mmol) was added to a 500 mL bottle. Solvents DMF (160 mL) and MeOH (27 mL) were added into the bottle and the bottle was capped. Its contents were then mixed for 10 min by a vortex mixer, sonicated for 10 min, and then placed in an 80 °C oven for 24 h to generate a yellow solution. After the solution was cooled down to room temperature, 0.7 mL of it was placed in a new 1 dram vial capped by aluminum foil, which was penetrated with 5 holes by a needle. After air evaporation (about two weeks), long, straight, rod-like, transparent, and colorless crystals were obtained.

Crystal 1B

Compound **1** (111 mg, 0.09 mmol) was dissolved in DMF (11.1 mL) with heating. After cooling down to room temperature, the mixture was filtered to produce a clear yellow solution. Then, 1 mL of this solution was placed in a new 2 dram vial, which was sealed with a cap. Yellow block-like crystals were generated within one day.

Data of Absorption and Emission Spectra in THF/H₂O

Table S1. Absorption and emission spectral data of **1** (10 μ M) in THF/H₂O with different H₂O volume percentages (f_w %).

f_w (%)	$\lambda_{\text{abs}}^{\text{a}}$ (nm)	$\lambda_{\text{em}}^{\text{a}}$ (nm)	I/I_0^{b}
0	298	410, 517	1.0
15	298	414, 514	1.6
30	298	410, 513	2.0
45	297	406, 512	2.4
60	296	404, 513	3.3
75	282, 393	507	29.6
90	281, 393	509	27.8
99	281, 392	507	27.3

[a] λ_{abs} and λ_{em} are the local maxima in absorption and emission spectra, respectively. [b] I is the integrated emission intensity from 300 to 700 nm.

Table S2. Absorption and emission spectral data of **2** (10 μ M) in THF/H₂O with different H₂O volume percentages (f_w %).

f_w (%)	$\lambda_{\text{abs}}^{\text{a}}$ (nm)	$\lambda_{\text{em}}^{\text{a}}$ (nm)	I/I_0^{b}
0	281	405, 515	1.0
15	281	407, 511	1.2
30	281	438, 497	1.8
45	285, 306	445	18.8
60	309	445	15.8
75	309	446	15.6
90	308	480	13.7
98	279	490	16.8

[a] λ_{abs} and λ_{em} are the local maxima in absorption and emission spectra, respectively. [b] I is the integrated emission intensity from 300 to 700 nm.

Photos and Excitation Spectra of Wetting/Drying Cycles

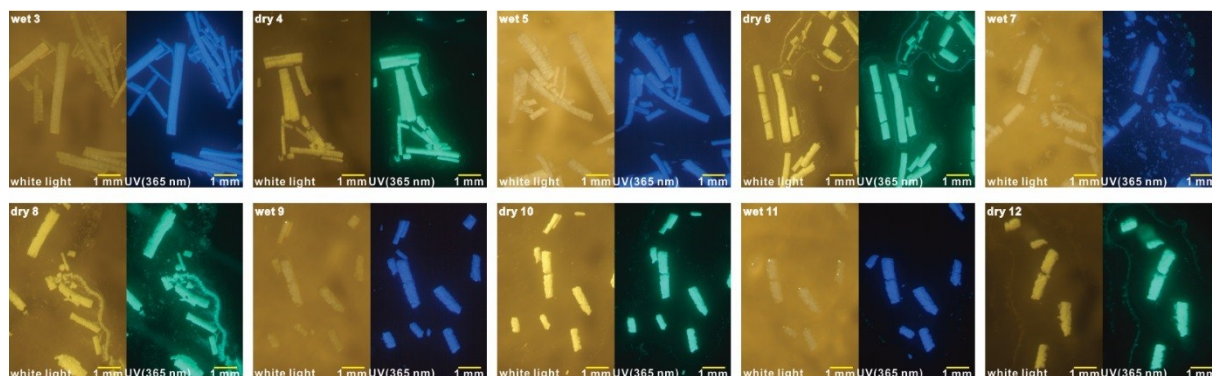


Figure S10. Digital microscope photos under white light (left in all panels) and UV ($\lambda_{exc} = 365$ nm, right in all panels) for the wetting/drying cycles (from “wet 3” to “dry 12”) of crystal 1A. Note: after the wetting/drying cycles, some of the test samples were lost gradually.

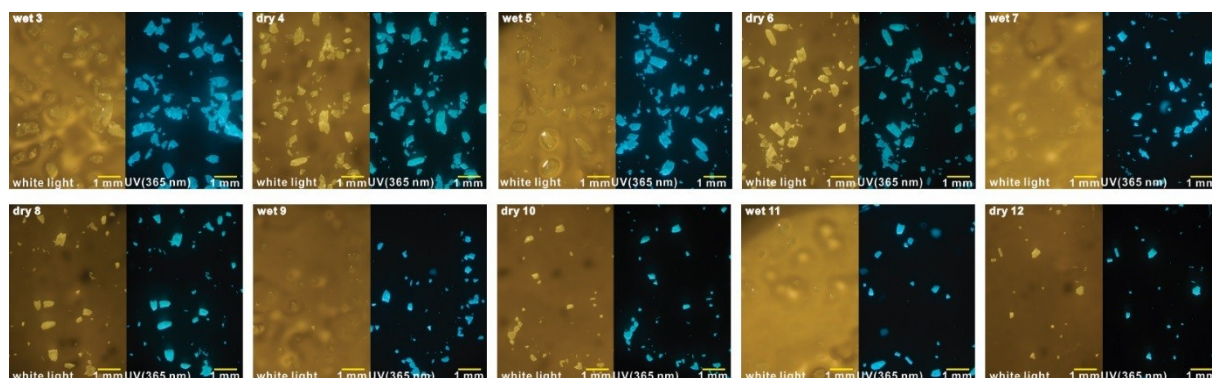


Figure S11. Digital microscope photos under white light (left in all panels) and UV ($\lambda_{exc} = 365$ nm, right in all panels) for the wetting/drying cycles (from “wet 3” to “dry 12”) of crystal 1B. Note: after the wetting/drying cycles, some of the test samples were lost gradually.

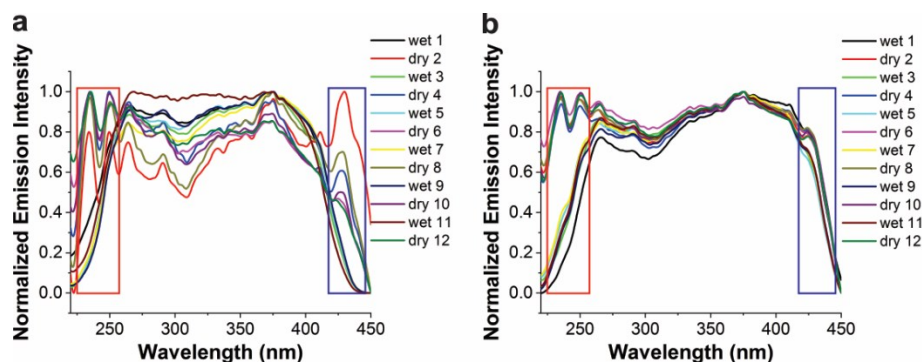


Figure S12. The excitation spectra ($\lambda_{em} = 478$ nm) of crystal **1A** (a) and **1B** (b) in wet and dry conditions.

The peaks around 235 and 250 nm under the dry conditions disappeared after wetting for both **1A** and **1B** (marked by red rectangles), which is due to the DMF's absorption under 270 nm that quenched the emission signals around 235 and 250 nm.³ The intensity of the new peak around 430 nm in the dried **1A** show an decrease tendency (marked by blue rectangle in Figure S9a), which may be due to the gradual damage of crystallinity of **1A** under the wetting-drying cycles (see Figure S7 and Figure S18). But the spectra of **1B** are almost overlapped at the long wavelength area (marked by blue rectangle in Figure S9b) for all the wet and dry conditions, which also suggests that **1B** is stable under such conditions.

Single and Powder X-ray Diffusion Analysis

All single X-ray diffraction measurements were performed by Dr. Xiqu Wang (UH) by using a Bruker DUO platform diffractometer equipped with a 4K CCD APEX II detector and an Incoatec 30 Watt Cu microsource with compact multilayer optics. Data were collected using a narrow-frame algorithm with scan widths of 0.50% in omega and an exposure time of 20 s per frame at 4 cm detector distance. The data were integrated using the Bruker SAINT program, with the intensities corrected for Lorentz factor, polarization, air absorption, and absorption due to the variation in the path length through the detector faceplate. The data were scaled, and an absorption correction was applied using SADABS. The structure was solved with SHELXT 2014, and refined with SHELXL 2014 using full-matrix least-squares refinement. The non-H atoms were refined with anisotropic thermal parameters, and all of the H atoms were calculated in idealized positions and refined riding on their parent atoms. The highly disordered solvent molecules could not be determined reliably and their contributions to the electron density were treated using the PLATON/SQUEEZE program. The chemical formulas and calculated density correspond to the ordered molecules only.

All powder X-ray diffraction measurements were performed on a Panalytical X'Pert Pro diffractometer.

Table S3. Crystal data and structure refinement for **1A** in wet condition.

Identification code	P108D_XW143_sq
Empirical formula	C ₆₈ H ₄₂ F ₁₆ N ₁₀ O ₂
Formula weight	1335.11
Temperature [K]	123(2)
Crystal system	monoclinic
Space group	C2/c
<i>a</i> [Å]	27.5164(10)
<i>b</i> [Å]	29.4938(10)
<i>c</i> [Å]	10.7214(4)
α [°]	90
β [°]	99.147(2)
γ [°]	90
Volume [Å ³]	8590.4(5)
<i>Z</i>	4
ρ_{calc} [g/cm ⁻³]	1.032
μ [mm ⁻¹]	0.766
<i>F</i> (000)	2720.0
Crystal size [mm ³]	0.500 × 0.120 × 0.010
Radiation	CuK α (λ = 1.54178 nm)
2 Θ range for data collection	4.422 to 133.572

[°]	
Index ranges	$-32 \leq h \leq 31, -34 \leq k \leq 35, -12 \leq l \leq 12$
Reflections collected	32028
Independent reflections	7570 [$R_{\text{int}} = 0.0420, R_{\text{sigma}} = 0.0333$]
Data/restraints/parameters	7570/0/436
Goodness-of-fit on F^2	1.026
Final R indexes [$I \geq 2\sigma(I)$]	$R_1 = 0.0548, wR_2 = 0.1631$
Final R indexes [all data]	$R_1 = 0.0637, wR_2 = 0.1735$
Largest diff. peak/hole [e \AA^{-3}]	0.42/-0.28

Table S4. Crystal data and structure refinement for **1B** in wet condition.

Identification code	P8-6_XW147
Empirical formula	$\text{C}_{74}\text{H}_{56}\text{F}_{16}\text{N}_{12}\text{O}_4$
Formula weight	1481.30
Temperature [K]	123(2)
Crystal system	triclinic
Space group	$P\bar{1}$
a [\AA]	17.4361(3)
b [\AA]	20.2383(4)
c [\AA]	21.2515(4)
α [°]	88.9760(10)
β [°]	72.8050(10)
γ [°]	70.2550(10)
Volume [\AA^3]	6714.7(2)
Z	4
ρ_{calc} [g/cm^{-3}]	1.465
μ [mm^{-1}]	1.069
$F(000)$	3040.0
Crystal size [mm^3]	$0.380 \times 0.310 \times 0.010$
Radiation	$\text{CuK}\alpha$ ($\lambda = 1.54178$)
2Θ range for data collection [°]	4.37 to 133.334
Index ranges	$-20 \leq h \leq 20, -24 \leq k \leq 24, -25 \leq l \leq 25$
Reflections collected	60699
Independent reflections	60699 [$R_{\text{int}} = 0.0476, R_{\text{sigma}} = 0.0641$]
Data/restraints/parameters	60699/1507/2135
Goodness-of-fit on F^2	1.033
Final R indexes [$I \geq 2\sigma(I)$]	$R_1 = 0.0669, wR_2 = 0.1771$
Final R indexes [all data]	$R_1 = 0.0917, wR_2 = 0.1994$
Largest diff. peak/hole [e \AA^{-3}]	0.89/-0.40

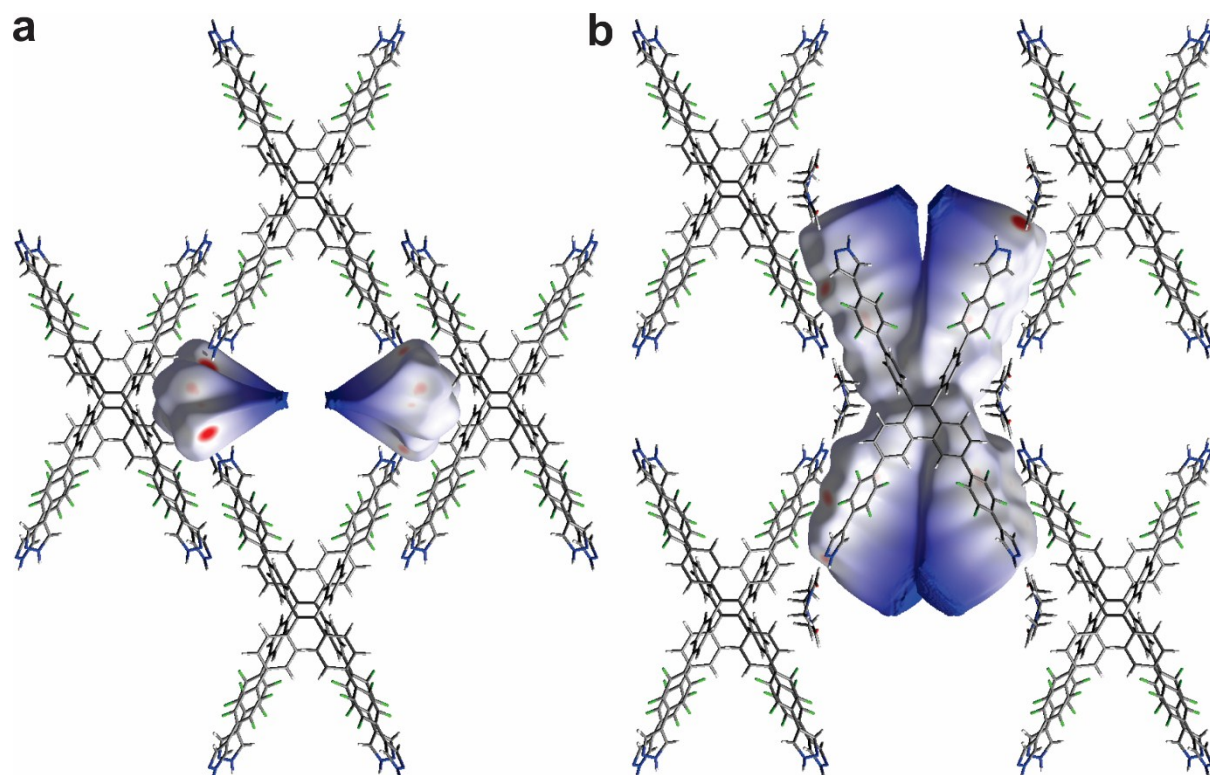


Figure 13. The Hirshfeld surfaces of DMF molecules (a) and a molecule of **1** (b) in single crystal **1A**

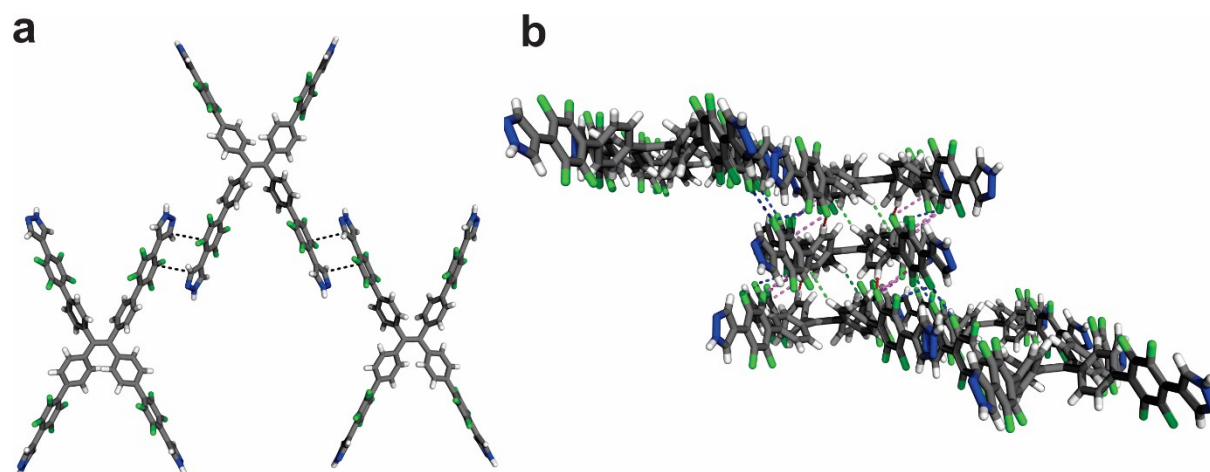


Figure 14. The intermolecular interactions of a molecule of **1** in single crystal **1A** established within a single layer (a), and between adjacent layers (b). Note: the green, black, red, blue, and violet dash lines in represent C···H, C···C, F···H, F···F, and C···F interactions, respectively.

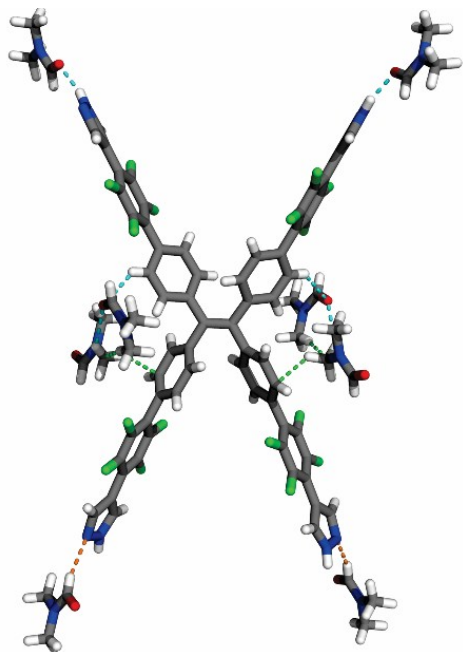


Figure S15. The interactions between **1** and DMF molecules in single crystal **1A**. Note: the cyan, orange, and green dash lines represent O···H, N···H, and C···H interactions, respectively.

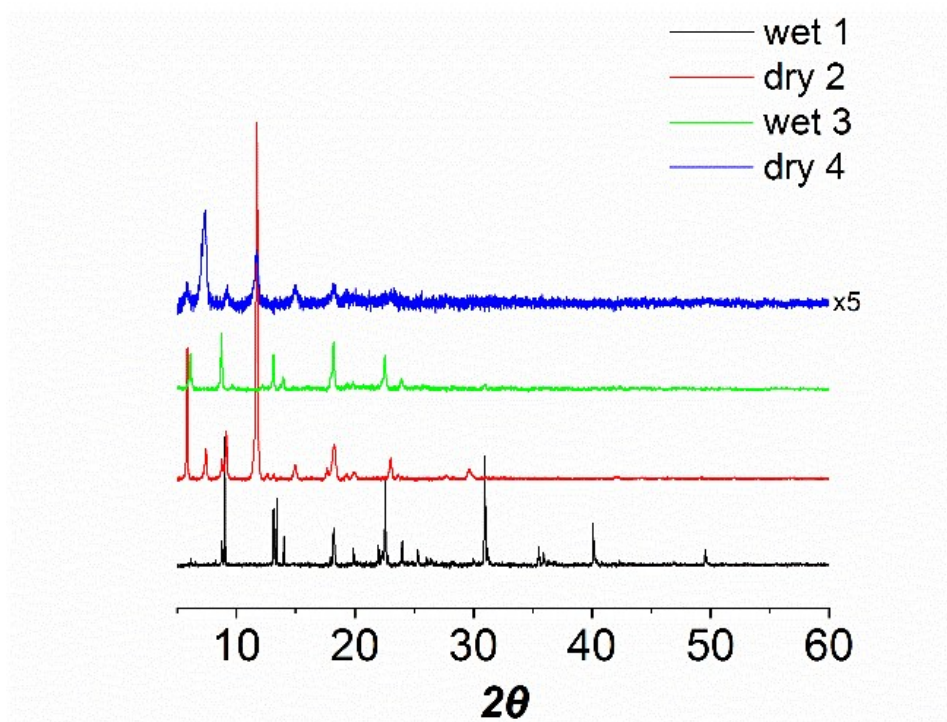


Figure S16. Powder XRD patterns for crystal **1A** following wetting and drying cycles. Note: the intensity of dry 4 is multiplied five times.

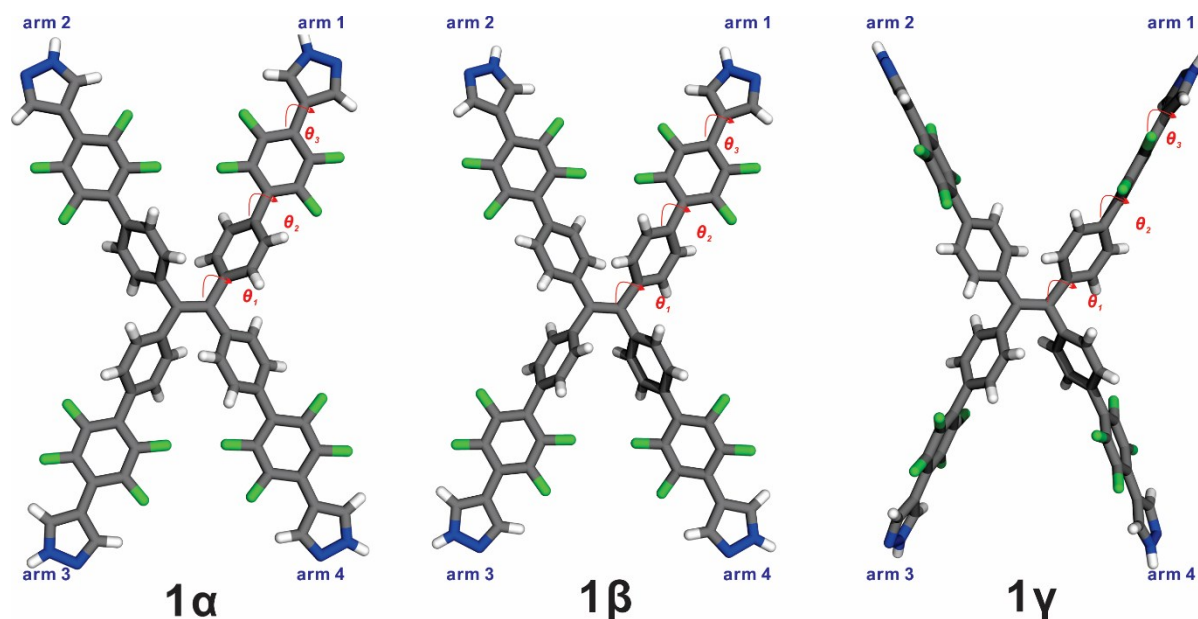


Figure S17. Three different conformations of molecules of **1** in single crystals **1B** (**1α** and **1β**) and **1A** (**1γ**). Note: θ_1 , θ_2 , and θ_3 are the dihedral angles between ethylene and benzene, benzene and tetrafluorobenzene, and tetrafluorobenzene and pyrazole moieties, respectively, in each arm.

Table S5. Dihedral angles^a in different conformations of **1** in single crystal **1A** and **1B**.

	1α of single crystal 1B				1β of single crystal 1B				1γ of single crystal 1A			
	θ_1 (°)	θ_2 (°)	θ_3 (°)	θ_4^b (°)	θ_1 (°)	θ_2 (°)	θ_3 (°)	θ_4^b (°)	θ_1 (°)	θ_2 (°)	θ_3 (°)	θ_4^b (°)
arm	44.6	53.2			50.0	56.2						
1	2	8	9.45	1.37	7	9	5.79	13.84	42.41	38.81	13.40	99.07
arm	48.1	44.1	11.9		43.8	44.8	29.9					
2	4	0	4	7.42	6	3	1	35.06	42.41	38.81	13.40	84.44
arm	47.9	52.3			53.0	50.7	10.2					
3	5	2	6.46	5.82	1	6	7	4.73	54.09	47.04	6.34	109.57
arm	41.1	46.6			52.9	41.7	24.3					
4	8	0	6.43	5.61	5	0	0	12.98	54.09	47.04	6.34	73.26

[a] all the dihedral angles are absolute values. [b] the θ_4 is the dihedral angles between ethylene and pyrazole in each arm, which are measured by the dihedral angle formed by C=C and N–N.

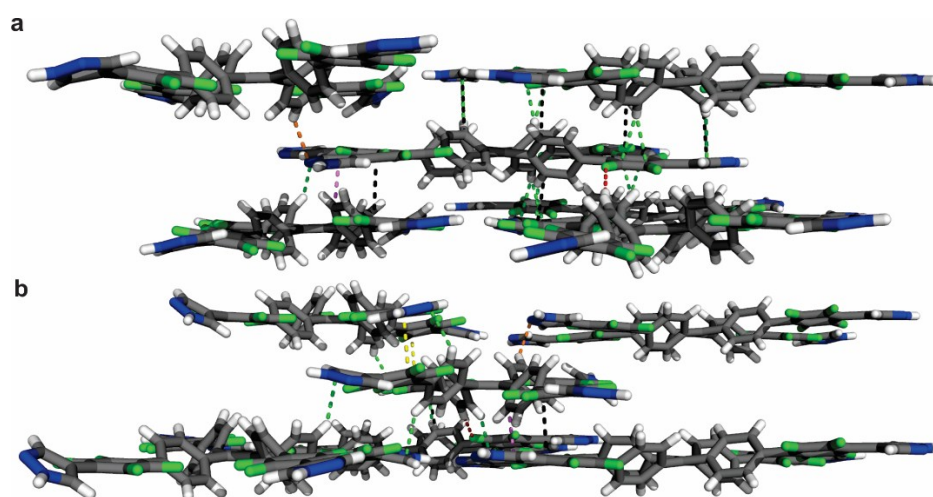


Figure S18. The intermolecular interactions in adjacent layers around unique molecules **1 α** (a) and **1 β** (b) in single crystal **1B**. Orange, green, black, yellow, red, and violet dashed lines represent N \cdots H, C \cdots H, C \cdots C, C \cdots N, F \cdots H, and C \cdots F interactions, respectively. Element colors: H—white, N—blue, C—gray, F—green, O—red.

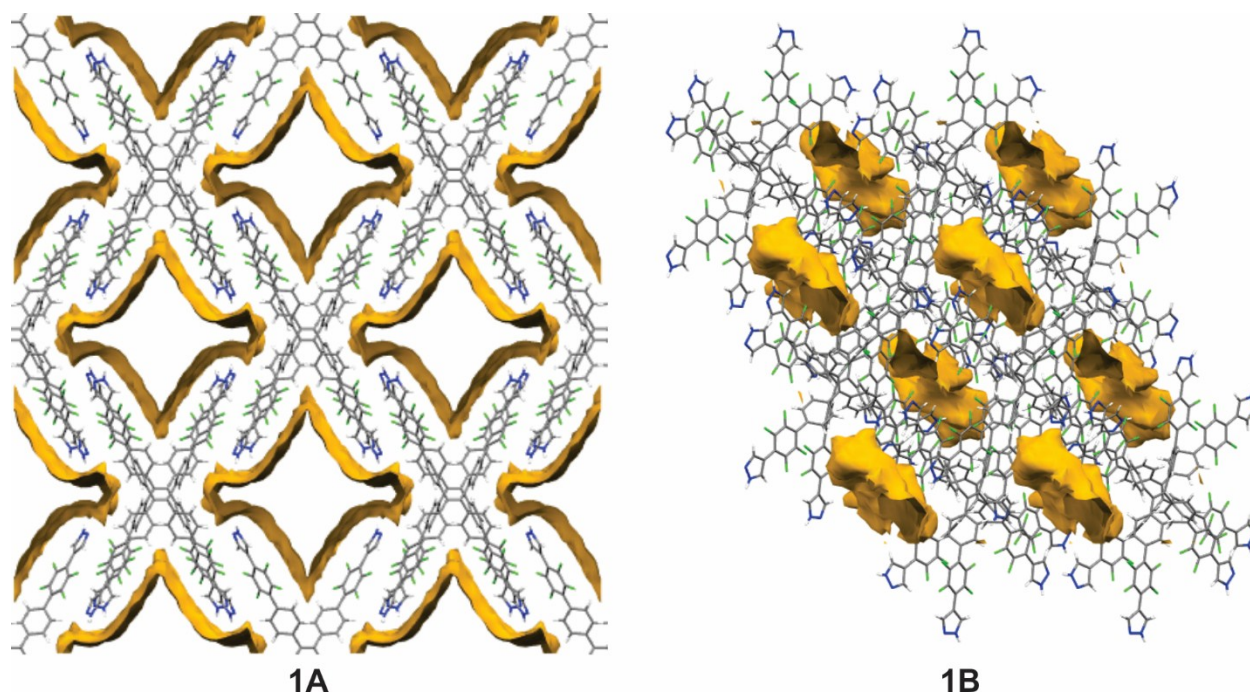


Figure S19. Void spaces in single crystal **1A** (2522.2 Å³, 29.4% of unit cell volume) and **1B** (527.0 Å³, 7.8% of unit cell volume) outlined with ochre contours as calculated by the solvent accessible surface method (probe radius = 1.2 Å, approx. grid spacing = 0.7 Å) as implemented in Mercury 4.0.0. Note: all the solvent molecules were removed for the calculation.

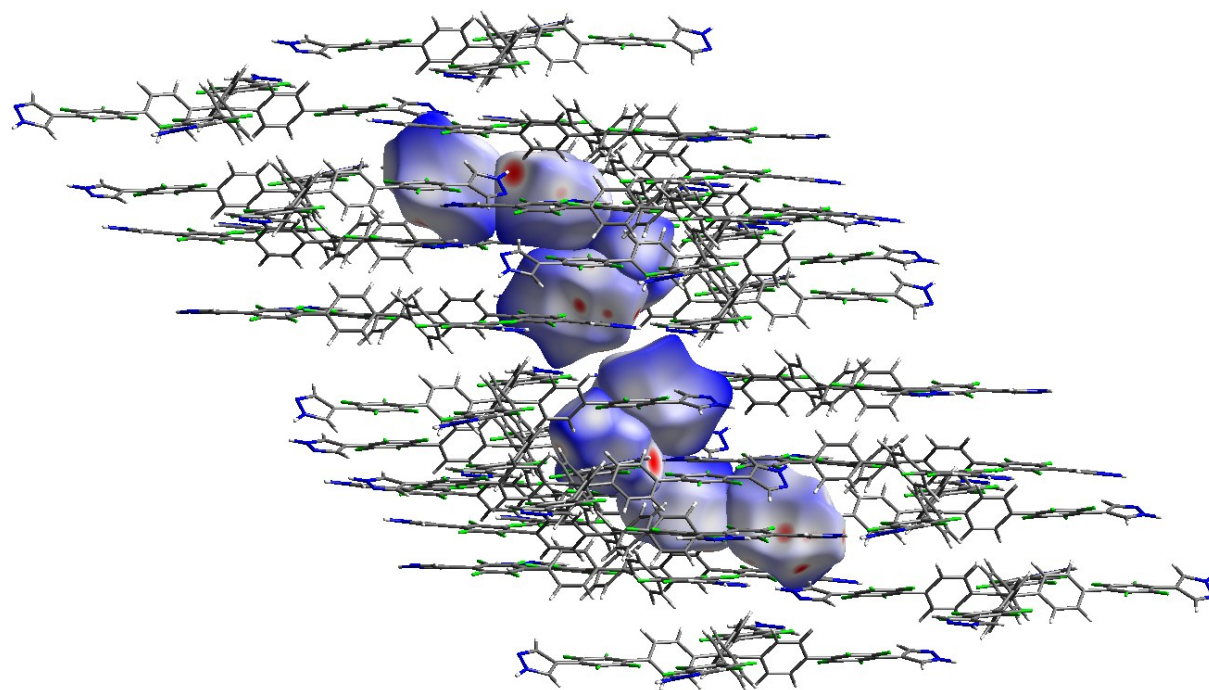


Figure S20. Eight molecules of DMF covered by Hirshfeld surface and the molecules of **1** around the DMF molecules in single crystal **1B**.

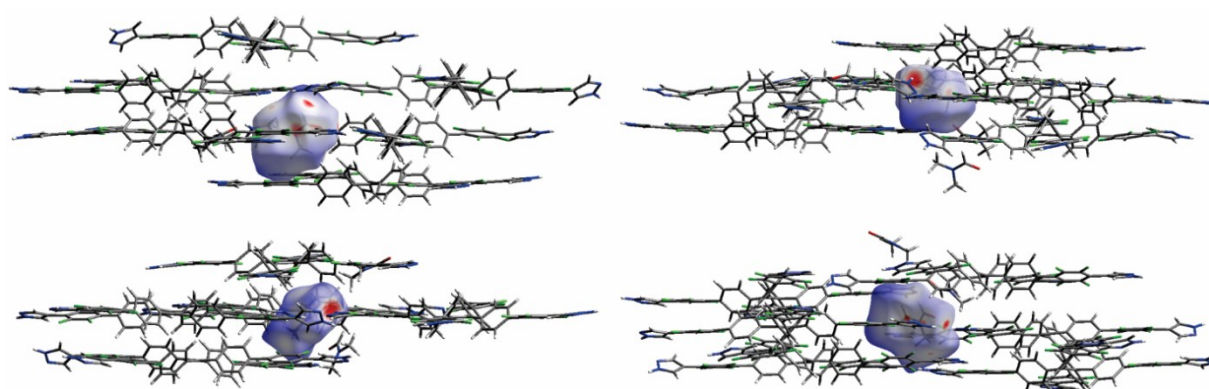


Figure S21. The Hirshfeld surfaces of four spatially close DMF molecules and the corresponding molecules around the surfaces in single crystal **1B**.

Theoretical Calculations

Energy Gaps between the Ground State and the First Excited State

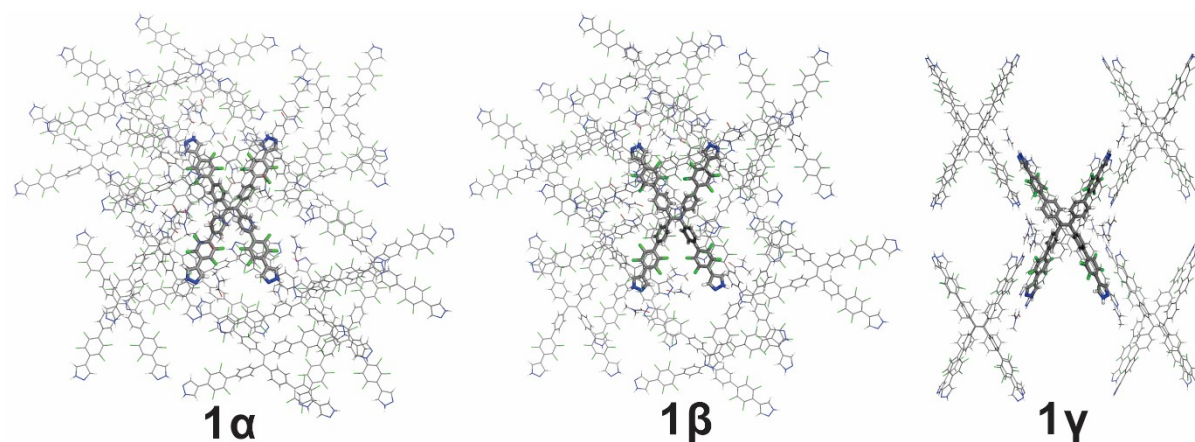


Figure S22. The input models based on Hirshfeld surface analyses of **1α** and **1β** in single crystal **1B** and **1γ** in single **1A**. Calculation settings: the setup of ONIOM model consists of two layers. The geometry optimizations were carried out for the high-level layer (stick molecules) using B3LYP/6-31G(d) for S_0 state and TD-B3LYP/6-31G(d) for S_1 state. The semiempirical method (PM6) was employed for the low-level layer (wireframe part) with fixed position (no structure optimized). Results of energy gap between S_1 and S_0 : $E(S_1)-E(S_0) = 2.52$ eV (492 nm), 2.51 eV (494 nm), and 2.74 eV (452 nm) and for **1α** and **1β** of **1B**, and **1γ** of **1A**, respectively. The calculations were carried out by Gaussian 16.⁴

References

- [1] T.-H. Chen, I. Popov, W. Kaveevivitchai, Y.-S. Chuang, Y. Chen, O. Daugulis, A. J. Jacobson, O. Š. Miljanić, *Nat. Commun.* **2014**, *5*, 14096.
- [2] Z. Wei, Z.-Y. Gu, R. K. Arvapally, Y.-P. Chen, R. N. McDougald Jr., J. F. Ivy, A. A. Yakovenko, D. Feng, M. A. Omary, H.-C. Zhou, *J. Am. Chem. Soc.* **2014**, *136*, 8269.
- [3] J. R. Rumble, ed., *CRC Handbook of Chemistry and Physics*, 99th Edition (Internet Version 2018), CRC Press/Taylor & Francis, Boca Raton, FL.
- [4] Gaussian 16, Revision A.03, M. J. Frisch, G. W. Trucks, H. B. Schlegel, G. E. Scuseria, M. A. Robb, J. R. Cheeseman, G. Scalmani, V. Barone, G. A. Petersson, H. Nakatsuji, X. Li, M. Caricato, A. V. Marenich, J. Bloino, B. G. Janesko, R. Gomperts, B. Mennucci, H. P. Hratchian, J. V. Ortiz, A. F. Izmaylov, J. L. Sonnenberg, D. Williams-Young, F. Ding, F. Lipparini, F. Egidi, J. Goings, B. Peng, A. Petrone, T. Henderson, D. Ranasinghe, V. G. Zakrzewski, J. Gao, N. Rega, G. Zheng, W. Liang, M. Hada, M. Ehara, K. Toyota, R. Fukuda, J. Hasegawa, M. Ishida, T. Nakajima, Y. Honda, O. Kitao, H. Nakai, T. Vreven, K. Throssell, J. A. Montgomery, Jr., J. E. Peralta, F. Ogliaro, M. J. Bearpark, J. J. Heyd, E. N. Brothers, K. N. Kudin, V. N. Staroverov, T. A. Keith, R. Kobayashi, J. Normand, K. Raghavachari, A. P. Rendell, J. C. Burant, S. S. Iyengar, J. Tomasi, M. Cossi, J. M. Millam, M. Klene, C. Adamo, R. Cammi, J. W. Ochterski, R. L. Martin, K. Morokuma, O. Farkas, J. B. Foresman, and D. J. Fox, Gaussian, Inc., Wallingford CT, 2016.